

## Chapter 10

# Infinite Networks of Hubs, Spirals, and Zig-Zag Patterns in Self-sustained Oscillations of a Tunnel Diode and of an Erbium-doped Fiber-ring Laser

Ricardo E. Francke, Thorsten Pöschel, and Jason A.C. Gallas

**Abstract.** A remarkably regular organization of spirals converging to a focal point in control parameter space was recently predicted and then observed in a nonlinear circuit containing two diodes. Such spiral organizations are relatively hard to observe experimentally because they usually emerge very compressed. Here we show that a circuit with a tunnel diode displays not one but two large spiral cascades. We show such cascades to exist over wide parameter ranges and, therefore, we expect them to be easier to observe experimentally.

### 10.1 Introduction

Numerical simulations have recently uncovered a number of surprising and unexpected regularities in the control parameter space of certain dissipative flows. Such regularities were observed in systems as diverse as electrical circuits containing either piecewise-linear or smooth nonlinearities, in certain lasers, in chemical oscillators and in several other paradigmatic flows covering a large spectrum of practical applications [1]– [21]. More specifically, a wide-ranging regular organization of

---

Ricardo E. Francke

Instituto de Física da UFRGS, 91501-970 Porto Alegre, Brazil

e-mail: ricardo.francke@ufrgs.br

Thorsten Pöschel · Jason A.C. Gallas

Institute for Multiscale Simulation, Friedrich-Alexander Universität,

D-91052 Erlangen, Germany

e-mail: Thorsten.Poeschel@cbi.uni-erlangen.de

Jason A.C. Gallas

Departamento de Física, Universidade Federal da Paraíba, 58051-970 João Pessoa, Brazil

Instituto de Física da UFRGS, 91501-970 Porto Alegre, Brazil

e-mail: jgallas@if.ufrgs.br

spirals was anticipated numerically to exist in the control parameter space of simple electronic circuit. This organization consists of a doubly infinite hierarchy of spirals converging to focal centers called “periodicity hubs” [2, 3]. Such hubs are very interesting accumulation points of a doubly infinite sequence of spirals: an infinite family of spirals characterized by periodic oscillations which is intercalated with an infinite family of spirals characterized by chaotic oscillations. Every periodic spiral has a characteristic waveform which evolves continuously along the spiral with a period that grows without any bound, diverging at the focal point. Loosely, hubs work like crowded bus stations with busses represent spirals: when arriving at such “station” following an *ingoing spiral* one is presented with a doubly-infinite choice for changing to an outgoing “bus”, i.e. to an *outgoing spiral*. This is so because there is an infinite choice of periodic as well as an infinite choice of chaotic patterns to choose from at the focal point. The selection may be simply accomplished by suitable selection of parameters. Examples of such hubs and spirals may be seen in Fig. 10.2 below. That the predicted spiral organization indeed exists in real systems was confirmed experimentally very recently at the ETH in Zürich [22] using a slight variation of the original circuit where they were numerically anticipated [2, 3]. Periodicity hubs were shown to be not isolated points but, instead, to emerge forming infinite hierarchical *networks of points* responsible for the organization of all stable periodic and chaotic phases [8].

Of particular interest for applications is that periodicity hubs are robust against parameter changes and imply a wide-range of predictable regularity in control parameter space. This is important because knowledge of the details of the regular organization of physical parameters allows one to select suitable numerical values to tailor the operation of circuits, lasers, and all sorts of nonlinear oscillators. By constructing detailed phase diagrams, i.e. by constructing detailed *stability charts* displaying the precise location in parameter space of the dynamical phases, one obtains a powerful instrument to perform accurate parameter changes allowing one to indeed *control* the system, not merely *to perturb* it without having a minimal ability of predicting in which new dynamic state the system will land after parameters are changed. Of course, parameter charts also allow one to perform big changes of control parameters, not just infinitesimally small changes.

So far, the spiral organization around periodicity hubs was observed in electronic circuits containing piecewise-linear elements [2–4, 22]. This type of circuits have two features that complicate experimental measurements. First, spirals usually emerge strongly distorted as, for example, in the paradigmatic circuit of Chua [3, 4]. Second, although it is known that spirals arise in infinite hierarchical networks [8], so far only a single isolated spiral has been detected experimentally [22].

The main reason complicating the observation of spiral networks is that the parameter regions containing them become significantly compressed making it hard to record them, particularly in noisy systems. An additional reason is that to observe networks one first needs to locate adequate two-parameter cuts in an usually high-dimensional control parameter space. This last task (parameter tuning) may

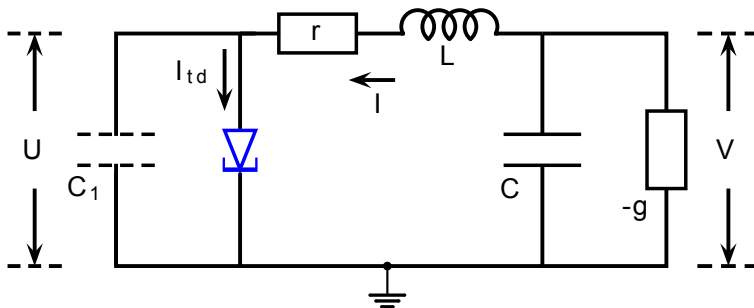


**Fig. 10.1** Schematic representation of the tunnel diode circuit leading to Eqs. (10.13)–(10.15). The voltage applied to the diode is denoted by  $U$ .

be rather difficult to perform experimentally. In this case computer simulations are of great help in locating suitable regions to search experimentally for hubs. On interesting additional byproduct is that computations may reveal shortcomings of the theoretical description of the electronic components (diodes, etc) in the sense that discrepancies between computations and measurements may emerge.

Here, our aim is to describe a simple autonomous electronic circuit, shown in Fig. 10.1, which we found to display clear and easily accessible sequences of spirals in its parameter space, as illustrated in Fig. 10.2 below. Apart from standard capacitances, inductances and resistances, the circuit contains two active elements, namely a linear negative conductance  $-g$  and a tunnel diode.

Chaotic oscillations in diodes were studied quite early in pioneering works by Pikovsky and Rabinovich [23–25] and other authors, e.g. [26]–[31], in several configurations, autonomous or not. Tunnel diodes were found to display very rich dynamical scenarios when their control parameters are varied [24, 26]. Although the chaotic dynamics of circuits with tunnel diodes seems nowadays to have simply felt in oblivion, we wish to point out that they contain an unsuspected richness of dynamics to offer both for convenient experimental exploration as well as to help developing novel theoretical tools to deal with new complex phenomena being discovered like, e.g. periodicity hubs, which are yet far from understood.

## 10.2 The Flow Defined by a Simple Circuit with a Tunnel Diode

In this Section we derive the equations governing the self-excited oscillator illustrated in Fig. 10.1, containing a tunnel diode. At the end of the Section we comment an approximation in the original expressions in the literature [24].

From Fig. 10.1, where  $I$  denotes the current through the inductance,  $U$  the voltage across  $C_1$ , and  $V$  the voltage across  $C$ , using Kirchhoff's laws we get:

$$V - U = rI + \frac{dI}{dt}, \quad (10.1)$$

$$-I = -gV + C \frac{dV}{dt}, \quad (10.2)$$

$$I = F(U) + C_1 \frac{dU}{dt}. \quad (10.3)$$

With the help of an auxiliary variable  $W \equiv V - rI$  these equations become

$$\frac{dI}{dt} = \frac{W - U}{L}, \quad (10.4)$$

$$\frac{dW}{dt} = -I \frac{1 - gr}{C} + \frac{gL - rC}{LC} W + \frac{r}{L} U, \quad (10.5)$$

$$\frac{dU}{dt} = \frac{I - F(U)}{C_1}. \quad (10.6)$$

Handy adimensional equations can be obtained by introducing the following changes of variable

$$\tau = \sqrt{\frac{1 - gr}{LC}} t \equiv \omega t, \quad I = (x + 1)I_0, \quad U = (z + 1)U_0, \quad y = \frac{W - U_0}{\omega L I_0}. \quad (10.7)$$

In addition, we need to replace  $F(U)$  by its transformed  $f(z)$  in the variable  $z$ , obtaining then:

$$\frac{dx}{d\tau} = y - \frac{U_0}{\omega I_0 L} z, \quad (10.8)$$

$$\frac{dy}{d\tau} = -x + \frac{gL - rC}{\omega LC} y + \frac{rU_0}{\omega^2 L^2 I_0} z + \left( -1 + \frac{gU_0}{\omega^2 I_0 LC} \right), \quad (10.9)$$

$$\frac{dz}{d\tau} = \frac{I_0}{\omega C_1 U_0} (x - f(z)). \quad (10.10)$$

Now, by introducing the following abbreviations

$$\delta = \frac{U_0}{\omega I_0 L}, \quad 2\gamma = \frac{gL - rC}{\omega LC}, \quad \alpha = \frac{rU_0}{\omega^2 L^2 I_0}, \quad (10.11)$$

$$\beta = -1 + \frac{gU_0}{\omega^2 I_0 LC} = \alpha - 1 + 2\gamma\delta, \quad \mu = \frac{\omega C_1 U_0}{I_0}, \quad (10.12)$$

the equations can be written in a much simpler form, namely,

$$\frac{dx}{d\tau} = y - \delta z, \quad (10.13)$$

$$\frac{dy}{d\tau} = -x + 2\gamma y + \alpha z + \beta, \quad (10.14)$$

$$\mu \frac{dz}{d\tau} = x - f(z). \quad (10.15)$$

These equations coincide with those of Pikovsky and Rabinovich [23–25]. However, we obtain them using  $\omega^2 = (1 - gr)/(LC)$  (see Eq. (10.7)) instead of the approximation  $\omega^2 = 1/(LC)$  used by them. Both expressions agree when  $gr \ll 1$ .

Equations (10.13)–(10.15) are used below to study the dynamics of the tunnel diode. In Eq. (10.15), the nonlinear function  $f(z)$  represents the characteristic function of the tunnel diode which, for simplicity, we assume to be a cubic function:  $f(z) \equiv z^3 - z$ .

Before proceeding we mention that Eqs. (10.13)–(10.15) were investigated theoretically in 1989 by Carcasses and Mira [32]. Using a Poincaré surface of section, these authors associated a two-dimensional diffeomorphism  $T$  to the differential equations and then considered the *qualitative* bifurcation structure of  $T$  in the  $\mu \times \beta$  parameter plane. Here, however, we consider the quantitative bifurcation structure observed in the  $\gamma \times \delta$  parameter plane as generated directly by Eqs. (10.13)–(10.15), not by an approximate Poincaré proxy.

### 10.3 The Slow-Fast Dynamics of the Circuit with a Tunnel Diode

Slow-fast systems (also known as singularly perturbed or systems with multiple time scales) are ubiquitous systems in physics, engineering, and biology in which two or more processes take place on different time scales [33, 34]. They are vector fields of the generic form

$$\mu \dot{x} = f(x, y, \mu), \quad (10.16)$$

$$\dot{y} = g(x, y, \mu), \quad (10.17)$$

where  $\mu$  is a small parameter.

In this context, the flow defined by Eqs. (10.13)–(10.15) is particularly interesting because the parameter  $\mu$  in front of the derivative  $\dot{z}$  may be conveniently tuned to induce dynamical effects happening at different time scales. When  $\mu$  is small, motions in the phase space can be divided into *slow motions*, corresponding to trajectories on the surface  $x = f(z)$ , and *fast motions*, corresponding to the straight lines  $x = \text{constant}$  and  $y = \text{constant}$ . As described by Rabinovich [24], the system has three states of equilibrium for a broad interval of values of the parameters  $\alpha, \beta, \gamma$ , and  $\delta$ , one state located at the origin, and the remaining pair located symmetrically on the surface of slow motions. All three states are unstable. If the untwisting of the paths near the unstable foci, say  $A$  and  $A'$ , is not too fast, the mapping point cannot leave the region containing all three states of equilibrium: the mapping point moves outward away from the point  $A$  along the spiral and, having reached the line  $x = \pm 1$  along which the surface of slow motion bends over, it enters the neighborhood of the symmetrically located state  $A'$ . It then follows the paths leaving this point thus returning to the neighborhood of  $A$ , repeating the sequence again and again.

An important property of flows like the one above is that two trajectories lying arbitrarily close to one another near the boundary at which they break off from the slow-motion surface, may behave completely differently. Those lying inside the path

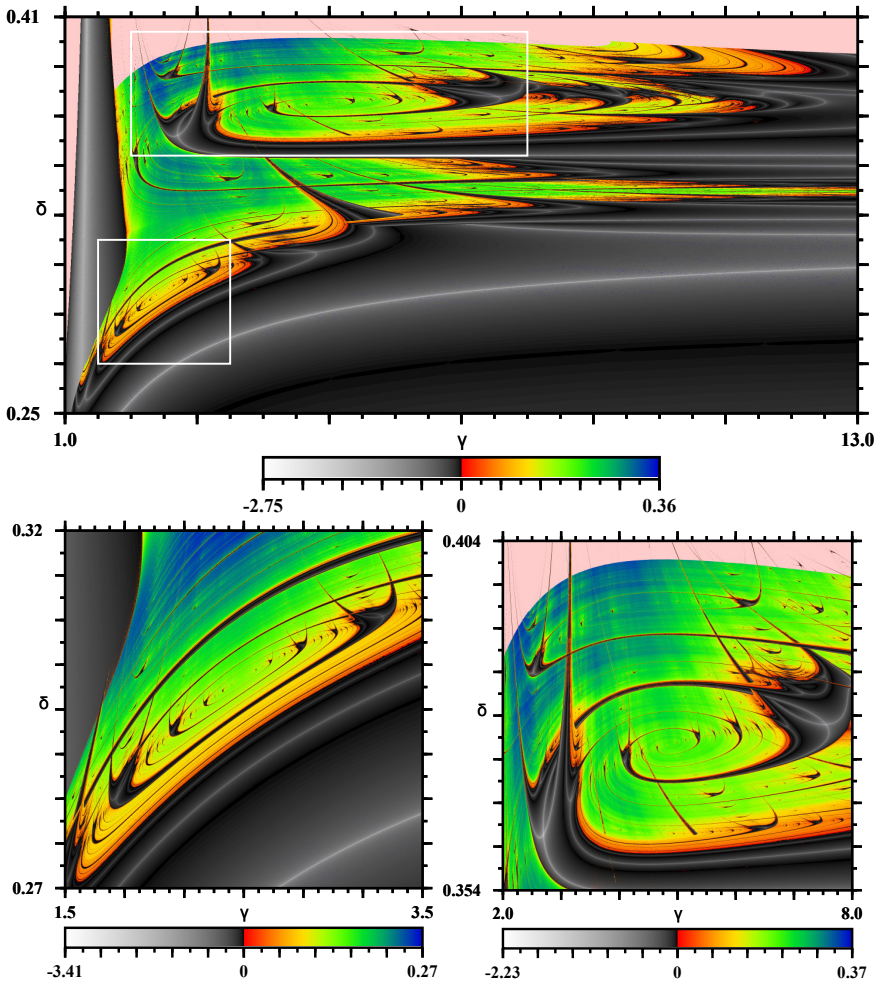


**Fig. 10.2** (Color online) Top panel: Global view of the control parameter space of the tunnel diode circuit, Eqs. (10.13)–(10.15), with boxes indicating the location of two periodicity hubs and spirals of large influence. Bottom panels: magnifications of the white boxes in the upper panel. Pink denotes divergent solutions. Here  $\alpha = -0.013$ ,  $\beta = 0$ ,  $\mu = 0.1$ . Each individual panel displays  $2400 \times 2400 = 5.76 \times 10^6$  Lyapunov exponents.

tangential to  $|x| = 1$  remain on the slow-motion surface and complete one additional turn around the equilibrium point. However, trajectories that are arbitrarily close to it but located outside this tangential path, fall downward (or rise upward) and enter the neighborhood of the symmetric state of equilibrium. Thus, as pointed out by Rabinovich [24], the future of these trajectories depends on fine details of their past.

Apart from  $f(z)$ , the flow defined by Eqs. (10.13)–(10.15) involves only linear terms, facilitating the theoretical analysis. Mathematically, the equations representing the circuit with a tunnel diode look quite similar to the ones governing the dynamics of the simple piecewise-linear resistive circuit where periodicity hubs were originally discovered [2, 3, 8]. Note that numerical simulations do not depend on the restriction of  $\mu$  being a small parameter.

## 10.4 Phase Diagrams

This Section presents several high-resolution Lyapunov phase diagrams discriminating the nature (chaotic or periodic) of the dynamical behavior observed in the  $\gamma \times \delta$  control parameter plane.

Lyapunov phase diagrams are generated by solving numerically the equations of motion (here with a standard fixed-step fourth-order Runge-Kutta integrator) and using the solutions obtained to compute all Lyapunov exponents for the system and plotting the largest nonzero exponent. As it is well-known, Lyapunov exponents are convenient numerical indicators used to discriminate the dynamical nature of the asymptotic oscillations observed in dynamical systems, i.e. they allow one to discriminate between periodic oscillations (which lead to negative exponents) and chaos (positive exponents).

Figure 10.2 shows Lyapunov phase diagrams summarizing what happens over a wide portion of the  $\gamma \times \delta$  control space of the tunnel diode, discriminating periodic from chaotic phases. As indicated by the color scales, colors represent positive Lyapunov exponents, i.e. regions where chaos is prevalent. In contrast, periodic phases are represented using darker shadings. Note that the color scales representing negative and positive exponents vary independently from each other on both sides of zero, i.e. the variation is not uniform from the negative minimum to the positive maximum of the scales. Further, the color table of each enlargement is renormalized according to the minimum and maximum exponents so that colors may vary as one magnifies specific regions of the parameter space.

In Fig. 10.2 it is possible to recognize something that is very desirable for experiments: the existence of two large-size groups of nested spirals accumulating into distinct focal points, where the periodicity hubs are located. Converging to each focal point one sees two groups of intertwined spirals, defined by periodic and by chaotic oscillations. Both groups seem to contain an infinite number of spirals. As parameters approach the focal point, the waveforms of the periodic oscillations evolve continuously and their periodicity grows without bound. Note that sequences of *shrimps* [35–37] occur along the periodicity spiral arranged in consecutive pairs at each half-turn. Many other interesting parameter domains worth investigating may be also recognized in Fig. 10.2. For details see Ref. [8].

In Fig. 10.2 and in other phase diagrams here we vary  $\gamma$  and  $\delta$  over experimentally accessible ranges. As it is clear from the definitions in Eqs. (10.11)–(10.12), specific values of  $\gamma$  and  $\delta$  may be conveniently achieved in more than one way by suitably selecting numerical values for the several reactances in the circuit. Thus, all circuit elements are equally important, not just the tunnel diode.

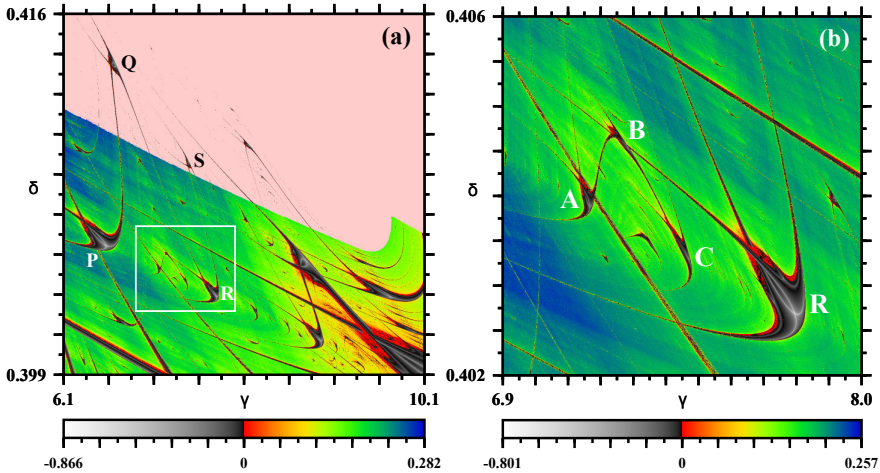


**Fig. 10.3** Examples of  $V$ -connections in the control space of the tunnel diode. (a) A zig-zag pattern  $PQRS$  formed by “gluing”  $V$ -connections together. The zig-zag continues beyond  $S$  but the additional shrimps are too small to be seen in the scale of the figure. Pink denotes parameter regions leading mainly to unbounded solutions (divergence); shrimps  $Q$  and  $S$  are embedded in it. (b) The  $V$ -connection  $ABC$  in the white box in (a). One of the legs of  $R$  allows passing between  $R$  and  $B$  via continuous parameter changes. A complex network of periodicity domains interconnects these shrimps. Here  $\alpha = -0.33, \beta = 0, \mu = 0.1$ .

Figure 10.3 shows a curious and abundant type of interconnection among distinct clusters of periodicity (“shrimps” [35]), computed here for  $\alpha = -0.33, \beta = 0, \mu = 0.1$ . Each panel of Fig. 10.3 shows  $1200 \times 1200$  Lyapunov exponents, the same resolution used in Figs. 10.5 and 10.6 below. Figure 10.3b displays an upside-down “ $V$ -connection” or “ $V$ -bridge”, as indicated by the letters  $ABC$ . This type of connection can be seen in Fig. 3 of a recent paper by Celestino et al. [15], who used a discrete map to study the properties of the unbiased current in the ratchet transport of particles. The shrimps in Fig. 10.3b are identical to those that combine to form the infinite chain that composes the continuous spirals in Fig. 10.2. Shrimps were originally described forming regular sequences of parallel clusters of periodicity, apparently disconnected from each other [36]. Here, however, the clusters of stability  $A$  and  $B$  are clearly interconnected by  $B$ , forming a structure that resembles an upside-down  $V$ . The periodicity clusters  $A, B$ , and  $C$  are contained in the white box in Fig. 10.3a which contains many such connections forming zig-zag sequences in parameter space.

As mentioned in the introduction, knowledge of the existence of such parameter paths interconnecting distinct clusters of periodicity may be obviously used as a simple and powerful technique to control the system, i.e. to efficiently implement with a single operation macroscopic parameter changes leading to desirable changes in the behavior of the system in a *predictable way*, allowing one to precisely select which change to implement. In sharp contrast to “control techniques” which rely

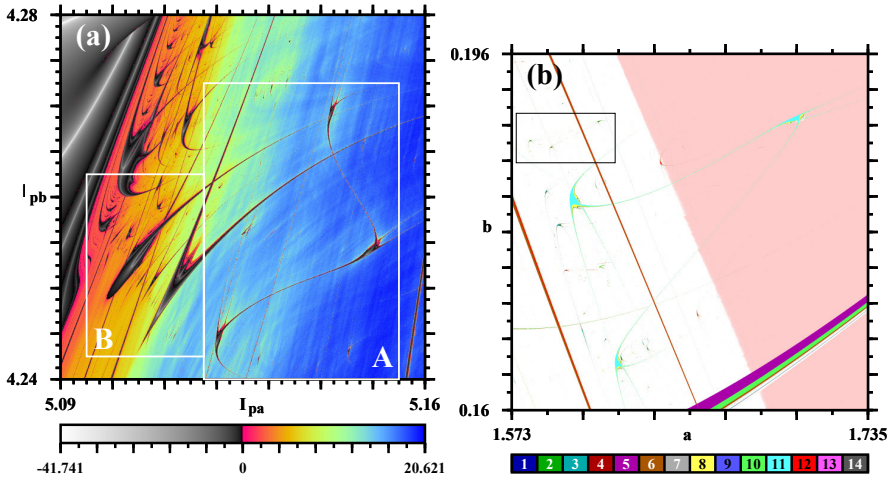


**Fig. 10.4** (Color online)  $V$ -connections observed in other systems. (a) in an erbium-doped fiber-ring laser (inside box A), and (b) in the discrete-time Hénon map of Eqs. (10.18)–(10.19). The two wide periodicity regions inside box B are high-order structures studied in detail for the Hénon map in Ref. [42]. The black box in (b) contains several additional  $V$ -connections which are too small to be seen in the scale of this figure [43]. Each panel displays results for  $2400 \times 2400$  parameter points. Pink denotes parameter regions leading mostly to divergence.

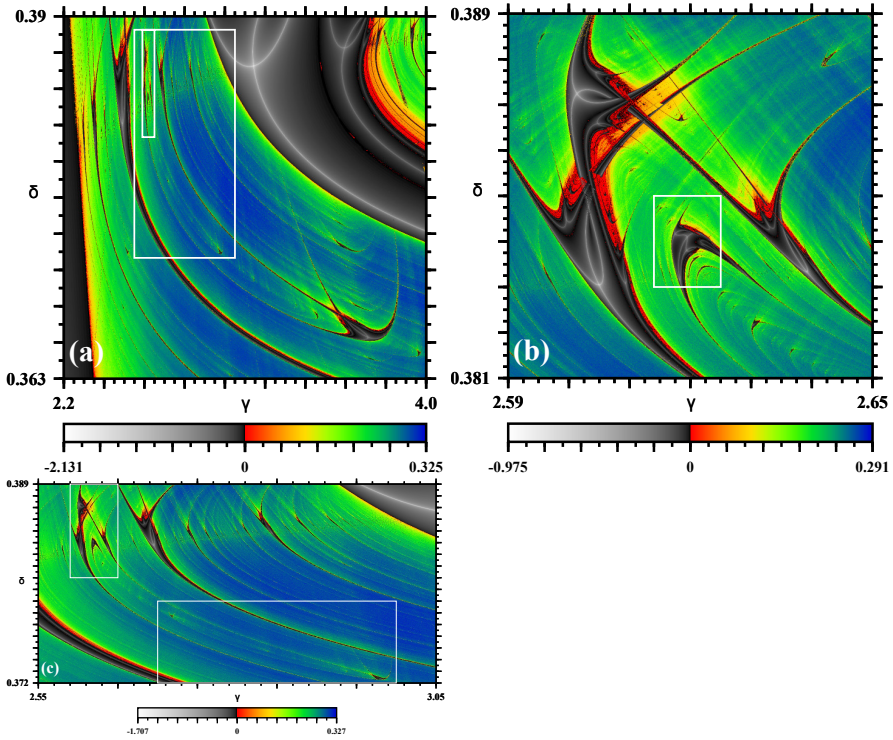
on infinitesimal changes and are totally unable to target any specific final orbit, knowledge of parameter charts allows one to perform parameter changes of any arbitrary size and may move to any nearby *stable* orbit either with a single parameter jump or with sequences of controlled parameter changes, if so desired.

Figure 10.4 shows that  $V$ -connection providing bridges among periodicity clusters are not difficult to find in other flows and even in the discrete-time models, i.e. in maps. For example, inside box A of Fig. 10.4a one sees a clear  $V$ -interconnection to be present in the control space of an erbium-doped dual-ring fiber laser [38–40]. Several others interconnections like this one exist over wide range of parameters [41]. The equations of motion and parameters adopted for this laser are given in the Appendix. Noteworthy in box B of this figure are the cuspidal island and the large island near it. Such structures appear profusely in parameter space. They have not been studied so far, although some results are known [42]. After the shrimps, the cuspidal island and the large island near it are the structures observed more frequently in the parameter space of flows and maps.

Figure 10.4b illustrates a  $V$ -connection for the paradigmatic discrete-time Hénon map defined here as follows [36, 37]:

$$x_{t+1} = a - x_t^2 + by_t, \tag{10.18}$$

$$y_{t+1} = x_t. \tag{10.19}$$



**Fig. 10.5** Successive enlargements illustrating a continuous spiral “arising” from a  $V$ -connection in the control space of the tunnel diode. (a) Global phase diagram, with the pair of boxes indicating the regions magnified in the other two panels. (b) The  $V$ -connection part of a spiral. The white box is magnified in Fig. 10.6. (c) Magnification of the largest box in (a), showing the  $V$ -connection (left box) and the spiral (inside the large white rectangle on the right). Several other analogous spirals and hubs exist although most of them are restricted to rather small parameter windows. Here  $\alpha = -0.33$ ,  $\beta = 0$ ,  $\mu = 0.1$ .

The Hénon map displays a profusion of  $V$ -connections, in addition to several other connections with complex forms that are quite difficult to classify systematically. The number of interconnections of all sorts is so great that one has the impression that in the end, all clusters of periodicity might in fact compose just a vast single network of connected domains fixed by the equations of motion. A more detailed investigation of the parameter space of the Hénon map is presented elsewhere [43].

Figure 10.5 illustrates a situation where, instead of the zig-zag patterns seen in Fig. 10.3, the  $V$ -connection gives origin to an infinite sequence of shrimps coiling up to form a continuous spiral. It seems appropriate to recall that a proper and encompassing mathematical description of spiral organizations in parameter space is still to be done. The only scenario that is presently reasonably well-understood is one associated with a theorem by L. Shilnikov [9, 10].

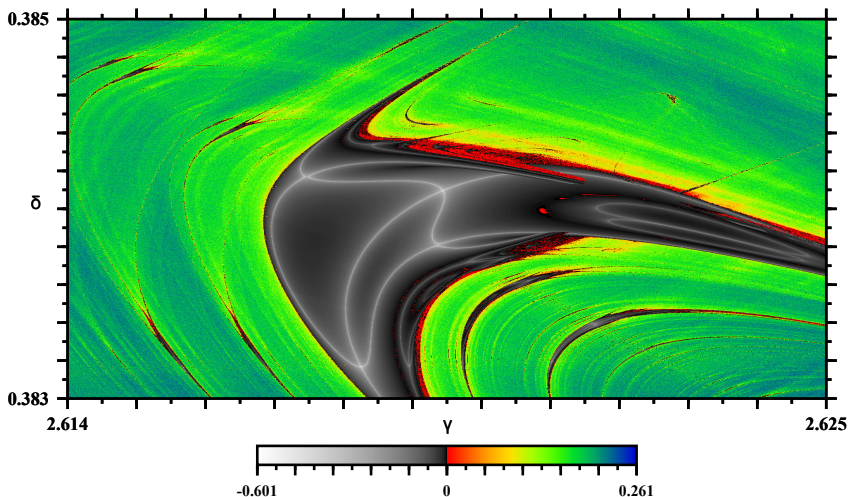


**Fig. 10.6** Magnification of the white box in Fig. 10.5b showing a complex periodicity cluster resembling a shrimp but containing a rather intricate network of loci that resemble “superstable” loci, a concept properly defined for one-dimensional multi-parameter maps. Here  $\alpha = -0.33, \beta = 0, \mu = 0.1$ .

However, considerably richer scenarios are possible in higher-dimensional slow-fast systems, particularly when period-doubling cascades follow a Hopf bifurcation and subsequent canard explosion, producing alternations of periodic and chaotic oscillations. As the amplitude of the chaotic attractors grows one observes a spiking regime consisting of large pulses separated by irregular time intervals in which the system displays small-amplitude chaotic oscillations. This scenario, reminiscent of Shilnikov’s homoclinic chaos despite the fact that no homoclinic connections are involved, has been observed very recently in ground-breaking experimental studies of a semiconductor laser with optoelectronic feedback by Al-Naimee et al. [44] and in the equations governing a light emitting diode (LED) subjected to the same feedback [45]. Such experiments provide new insight, showing that key concept of excitability needs to be extended beyond that familiar to fixed points, into the realm of higher-dimensional attractors of maps and flows as anticipated theoretically [46]. They equally show that slow-fast systems are relatively poorly understood and need to be investigated in more detail. Interestingly, lasers and circuits with LEDs open now the possibility for probing experimentally such elusive and unexplored phenomena. For details, see Refs. [7, 45].

Figure 10.6 displays a structure that looks like a shrimp but contains a much more intricate arrangement of parameters as represented by the white curves inside the wide periodicity cluster. Such curves look very much like “superstable loci”. However, as pointed before [2], superstable loci are only defined for one-dimensional maps, where they mark trajectories passing through at least one “critical point” of the map, i.e. a point where the derivative of the map is zero [47]. Although Fig. 10.6

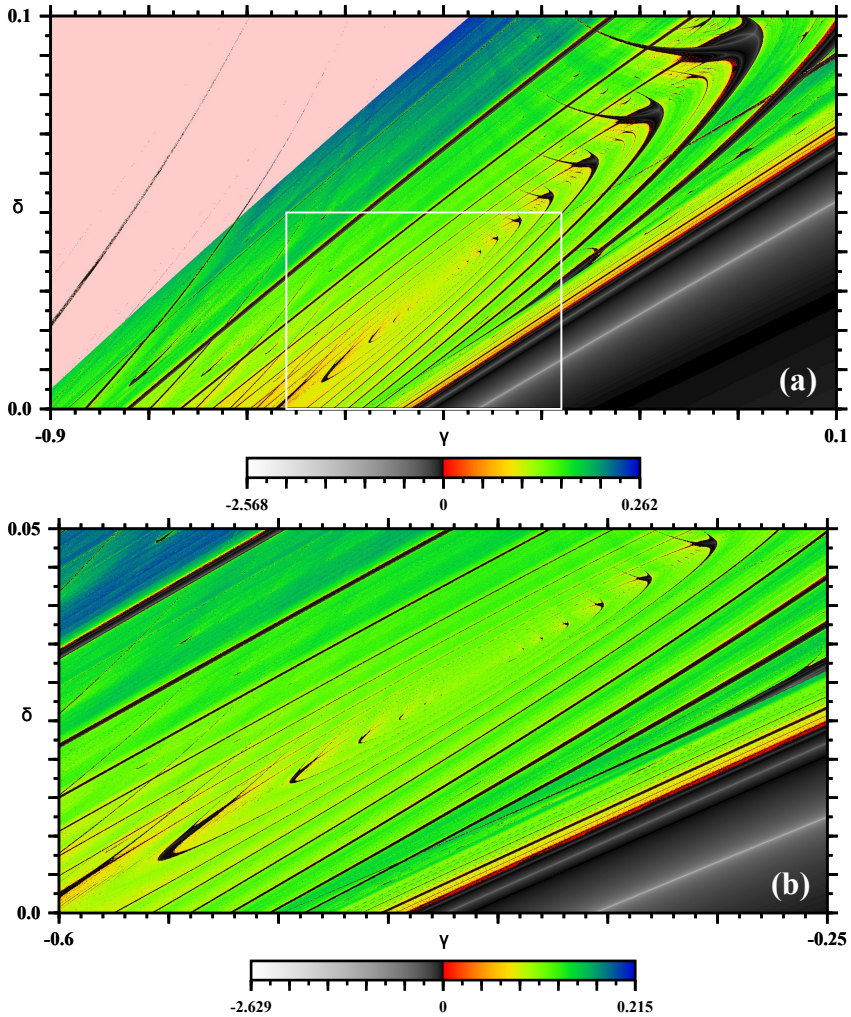


**Fig. 10.7** Illustration of a spiral structure extending over a very wide parameter range of the tunnel diode. Similar spiral arrangements exist over wide ranges for many other choices of parameters. This structure of the parameter space looks quite similar to the one found in the control space of Chua’s circuit [3, 4, 8]. Each panel displays  $1600 \times 1600 = 2.56 \times 10^6$  Lyapunov exponents. Here  $\alpha = -0.33, \beta = 0, \mu = 0.1$ .

displays a phase diagram for a flow (not a map), for lack of a proper definition and a better name we loosely refer to the white curves as being “superstable loci”. Two important points may be recognized from Fig. 10.6: first, the existence of rather complex periodicity clusters not yet considered theoretically and, second, the necessity of adequately generalizing some known concepts in order to also deal with pressing situations that emerge abundantly when considering periodicity clusters of

flows. We remark that even though stability diagrams for flows display rather interesting networks of the aforementioned “superstable loci”, there is still no theoretical prescription which would allow one to predict their existence and compute them for flows. In fact, even a proper name is still to be invented for them.

Figure 10.7 displays spiral structures which extend over very wide parameter ranges and that, we believe, should be relatively easy to observe in experiments. Of course, experimental resolution sets a limit on the number of turns of the spiral that can be observed. Important here is that the regular distribution of the successive shrimps gives an indication that a spiral has been spotted. For instance, it should not be difficult to unveil the regular organization simply by plotting bifurcation diagrams passing through the diagonal line containing the main body of the shrimps. The spiral organization seen in Fig. 10.7 looks very similar to spirals reported for Chua’s circuit when operating both with piecewise-linear or cubic nonlinearities, as might be seen from Fig. 4 of Ref. [4] or from Fig. 5 of Ref. [8]. How could one objectively quantify the isomorphism among these systems?

## 10.5 Conclusions and Outlook

This work presented several high-resolution Lyapunov phase diagrams showing that a simple circuit containing a tunnel diode displays a pair of large continuous spiral networks with rich intertwined structures extending over a wide region in control parameter space. Near them one finds an infinite sequence of smaller spirals, as described in Refs. [8, 9]. The large pair of spiral networks makes tunnel diodes quite interesting testground to probe experimentally intricate and elusive dynamical properties described recently in the literature. We also described the abundance of a class of shrimp arrangement, certain  $V$ -connections [15], which we have shown to be capable of forming quite long zig-zag paths and networks in parameter space. Analogous features were also observed in the control space of an erbium-doped dual-ring fiber laser and of the much simpler Hénon map, known to represent well the dynamics of loss-modulated CO<sub>2</sub> lasers [1]. Spirals and zig-zag patterns offer an interesting way to move in a *controlled and systematic way* between families of stable solutions, quite distinct from the nowadays so popular method of randomly perturbing trajectories without having any control of the final state to be reached after application of the perturbation.

Parameter spirals of periodicity (and of chaoticity) emerge from and accumulate at periodicity hubs: mathematically, such hubs are associated in phase-space with very small regions of quite strong curvature, sometimes (but not necessarily) involving homoclinic bifurcation curves of a common saddle-focus equilibrium. These homoclinic bifurcation curves are arranged in fractal-like sheaves in the parameter plane [9]. The specific organization of hub networks *depends strongly on the interaction between the homoclinic orbits and the global structure of the underlying attractor* [9]. A challenging problem now is to describe what is causing the complex organization of periodicity clusters in phase diagrams of flows not involving homoclinic orbits. Note that presently there is no mathematical framework to predict and

describe the genesis of hubs and the associated spirals in more general scenarios where the celebrated theorem of Shilnikov does not apply [7, 9].

The present work also shows that Lyapunov phase diagrams are quite valuable exploratory tools for practical applications allowing one to understand global features of complex attractors. We believe that the use of Lyapunov phase diagrams can significantly augment and speed-up the understanding of physical models. Lyapunov phase diagrams focus exclusively on *stable solutions*, i.e. on features that are directly measurable experimentally. Lyapunov phase diagrams reveal the occurrence of many global bifurcations without recourse to more specialized and demanding numerical techniques. They are therefore a very powerful way to begin the analysis of nonlinear systems and can also be applied to laboratory experiments which, of course, only detect stable structures. As described elsewhere in detail [7], note that *there is absolutely no need to compute Lyapunov exponents from experimentally measured data*. For experimental data it is enough to simply construct “binary” black-and-white phase diagrams discriminating between two states: presence or absence of periodicity. A complementary tool of great utility in analyzing dynamical systems is the direct study of the *periodicity and the number of extrema of the oscillations* as parameters are tuned [48, 49] (without recourse to secondary and somewhat artificial quantities derived from the period like, e.g. when artificially introducing *pairs* of frequencies in phenomena where such pairs are not naturally present or not quite justifiable [49, 50]).

We hope the findings reported here to motivate their experimental investigation. From a theoretical point of view, at present it is totally unclear where to expect hubs and spirals to be found in flows. It is equally unclear which type of flows should be expected to contain hubs and spirals, particularly in high-dimensional systems. Thus, the only way to learn about them is through detailed numerical simulations and experiments. A related open question is how to optimize the search for the “most convenient” sections of the high-dimensional surface in control parameter space so as to better expose the intricacies and the structure of phase diagrams. In other words, to find an efficient way of quickly asserting the impact of changing *all control parameters*. From an experimental point of view, an interesting challenge is to investigate how realistic the simple cubic function used here is to describe the dynamics of real-life tunnel diodes. Obviously, high-resolution phase diagrams have the power of revealing eventual shortcomings of the mathematical formulation of models of natural phenomena. Phase diagrams can show where models need to be improved to better reproduce experimental measurements.

**Acknowledgements.** We are indebted to Arkady Pikovsky for helpful email exchanges concerning certain approximations that they used to obtain their equations. This work was supported by the Deutsche Forschungsgemeinschaft through the Cluster of Excellence *Engineering of Advanced Materials*. JACG was supported by CNPq, Brazil, and by the US Air Force Office of Scientific Research, Grant FA9550-07-1-0102. All computations were done in the CESUP-UFRGS clusters. A preliminary version of these results was presented at the *Workshop on Nonlinear Physics and Applications*, NOLPA, in João Pessoa, Brazil, September 5-9, 2011.

## References

1. Bonatto, C., Garreau, J.C., Gallas, J.A.C.: Phys. Rev. Lett. 95, 143905 (2005)
2. Bonatto, C., Gallas, J.A.C.: Phys. Rev. Lett. 101, 054101 (2008); Phil. Trans. Royal Soc. London, Series A 366, 505 (2008)
3. Ramírez-Ávila, G.M., Gallas, J.A.C.: Revista Boliviana de Física 14, 1–9 (2008)
4. Ramírez-Ávila, G.M., Gallas, J.A.C.: Phys. Lett. A 375, 143 (2010)
5. Freire, J.G., Field, R.J., Gallas, J.A.C.: J. Chem. Phys. 131, 044105 (2009)
6. Kovanis, V., Gavrielides, A., Gallas, J.A.C.: Eur. Phys. J. D 58, 181 (2010)
7. Freire, J.G., Gallas, J.A.C.: Phys. Rev. E 82, 037202 (2010)
8. Gallas, J.A.C.: Int. J. Bif. Chaos 20, 197 (2010)
9. Vitolo, R., Glendinning, P., Gallas, J.A.C.: Phys. Rev. E 84, 016216 (2011)
10. Barrio, R., Blesa, F., Serrano, S., Shilnikov, A.: Phys. Rev. E 84, 035201(R) (2011)
11. Bragard, J., Pleiner, H., Suarez, O.J., Vargas, P., Gallas, J.A.C., Laroze, D.: Phys. Rev. E 84, 037202 (2011)
12. Castro, V., Monti, M., Pardo, W.B., Walkenstein, J.A., Rosa Jr., E.: Int. J. Bif. Chaos 17, 956 (2007)
13. Zou, Y., Thiel, M., Romano, M.V., Kurths, J., Bi, Q.: Int. J. Bif. Chaos 16, 3567 (2006)
14. Albuquerque, H.A., Rubinger, R.M., Rech, P.C.: Phys. Lett. A 372, 4793 (2008)
15. Celestino, A., Manchein, C., Albuquerque, H.A., Beims, M.W.: Phys. Rev. Lett. 106, 234101 (2011)
16. Oliveira, D.F.M., Robnik, M., Leonel, E.D.: Chaos 21, 043122 (2011)
17. Oliveira, D.F.M., Leonel, E.D.: New J. Phys. 13, 123012 (2011)
18. Stegemann, C., Albuquerque, H.A., Rubinger, R.M., Rech, P.C.: Chaos 21, 033105 (2011)
19. Stegemann, C., Albuquerque, H.A., Rech, P.C.: Chaos 20, 023103 (2010)
20. Viana, E.V., Rubinger, R.M., Albuquerque, H.A., de Oliveira, A.G., Ribeiro, G.M.: Chaos 20, 023110 (2010)
21. Cardoso, J.C.D., Albuquerque, H.A., Rubinger, R.M.: Phys. Lett. A 373, 2050 (2009)
22. Stoop, R., Benner, P., Uwate, Y.: Phys. Rev. Lett. 105, 074102 (2010)
23. Pikovsky, A.S., Rabinovich, M.: Sov. Phys. Dokl. 23, 183 (1978); Dokl. Akad. Nauk SSSR 239, 301–304 (1978)
24. Rabinovich, M.: Sov. Phys. Usp. 21, 443–469 (1978); Usp. Fiz. Nauk 125, 123–168 (1978)
25. Pikovsky, A.S., Rabinovich, M.: Physica D 2, 8 (1981)
26. Gollub, J.P., Brunner, T.O., Daly, B.G.: Science 200, 48 (1978)
27. Gollub, J.P., Romer, E.J., Socolar, J.E.: J. Stat. Phys. 23, 321 (1980)
28. Linsay, P.S.: Phys. Rev. Lett. 47, 1349 (1981)
29. Testa, J., Perez, J., Jeffries, C.: Phys. Rev. Lett. 48, 714 (1982)
30. Octavio, M., DaCosta, A., Aponte, J.: Phys. Rev. A 34, 1512 (1986)
31. Su, Z., Rollins, R.W., Hunt, E.R.: Phys. Rev. A 40, 2698 (1990)
32. Carcasses, J.P., Mira, C.: In: Mira, C., Netzer, N., Simo, C., Targonski, G. (eds.) Proc. Int. Conf. on Iteration Theory: ECIT 1989, Batschuns, World Scientific, Singapore (1991)
33. Jones, C.K.R.T., Khibnik, A.I.: Multiple-Time-Scale Dynamical Systems, Mathematics and its Applications, vol. 122. Springer, NY (2000)
34. Grasman, J.: Asymptotic methods for relaxation oscillations and applications, Applied Mathematical Sciences, vol. 63. Springer, NY (1987)

35. “Shrimps” refer to wide-reaching structures in parameter space formed by a regular set of adjacent windows centered around a main pair of usually intersecting ‘superstable’ parabolic arcs (see discussion of Fig. 9.6). Thus, a shrimp is a doubly-infinite *mosaic of periodicity domains* composed by an innermost *main* domain plus all the adjacent periodicity domains arising from two symmetrically located period-doubling cascades together with their corresponding domains of chaos [36]. Shrimps should not be confused with their innermost main domain of periodicity or with superstable loci. For details see Refs. [36, 37]
36. Gallas, J.A.C.: Phys. Rev. Lett. 70, 2714 (1993); Physica A 202, 196(1994); Appl. Phys. B 60, S203 (1995), special supplement issue: Festschrift Herbert Walther; Hunt, B.R., Gallas, J.A.C., Grebogi, C., Yorke, J.A., Koçak, H.: Physica D 129, 35(1999)
37. Lorenz, E.N.: Physica D 237, 1689 (2008)
38. Luo, L., Tee, T.J., Chu, P.L.: J. Opt. Soc. Am. B 15, 972 (1998)
39. Senlin, Y.: Chaos 17, 013106 (2007)
40. Zhang, S., Shen, K.: Chin. Phys. 12, 149 (2003)
41. Pöschel, T., Gallas, J.A.C.: The distribution of self-pulsing and chaos in control space of an erbium-doped fiber-ring laser, preprint
42. Endler, A., Gallas, J.A.C.: Comptes Rendus Mathem (Paris) 342, 681 (2006)
43. Gallas, J.A.C.: Shrimps and the eigenvalue structure of the Hénon map, preprint
44. Al-Naimee, K., Marino, F., Ciszak, M., Abdalah, S.F., Meucci, R., Arecchi, F.T.: Eur. Phys. J. D 58, 187 (2010); New J. Phys. 11, 073022 (2009)
45. Marino, F., Ciszak, M., Abdalah, S.F., Al-Naimee, K., Meucci, R., Arecchi, F.T.: Phys. Rev. E 84, 047201 (2011)
46. Marino, F., Marin, F., Balle, S., Piro, O.: Phys. Rev. Lett. 98, 074104 (2007)
47. For a quite early and very nice review of the role of critical points as originally used by Schröder, Fatou and Julia, see H. Cremer, Jahresber. Deutsche Math. Ver. 33,185 (1924)
48. Freire, J.G., Gallas, J.A.C.: Phys. Lett. A 375, 1097 (2011)
49. Freire, J.G., Gallas, J.A.C.: Phys. Chem. Chem. Phys. 13, 12191 (2011)
50. Freire, J.G., Pöschel, T., Gallas, J.A.C.: Stern-Brocot tree: A unifying organization of oscillations for a broad class of phenomena, submitted for publication

## Appendix: The Erbium-Doped Dual-Ring Fiber Laser

This Appendix collects the equations for the continuous-time model of the erbium-doped dual-ring fiber laser.

We follow Luo et al. [38] and consider the erbium-doped dual-ring fiber laser with the lasing fields in the two rings frequency locked through a coupler  $c_0$  with phase change of  $\pi/2$  from one ring to the other. In this case, the equations for the fundamental system are [38–40]:

$$\frac{dE_a}{dt} = -k_a(E_a + c_0E_b) + g_aE_aD_a, \quad (10.20)$$

$$\frac{dE_b}{dt} = -k_b(E_b - c_0E_a) + g_bE_bD_b, \quad (10.21)$$

$$\frac{dD_a}{dt} = -(1 + I_{pa} + E_a^2)D_a + I_{pa} - 1, \quad (10.22)$$

$$\frac{dD_b}{dt} = -(1 + I_{pb} + E_b^2)D_b + I_{pb} - 1, \quad (10.23)$$

where  $E_a$  and  $E_b$  are the lasing fields and  $D_a$  and  $D_b$  are the population inversion in rings  $a$  and  $b$ , respectively. The parameters  $k_a, k_b, g_a, g_b$  represent the decay rate and the gain coefficient of the lasing fields  $a$  and  $b$ , as indicated.  $I_{pa}$  and  $I_{pb}$  represent pump intensity in the respective fiber rings. Note that this laser model contains cubic nonlinearities, similarly to the one present in the tunnel diode model.

For the model above, an interesting paper by Zhang and Shen [40] reported hyperchaotic dynamics, in particular for the following set parameters

$$k_a = k_b = 1000, \quad c_0 = 0.2, \quad g_a = 10500, \quad g_b = 4700.$$

These are the parameter values adopted here to compute the phase diagram in Fig. 10.4. However, we emphasize that the laser phase diagram is not at all sensitive to these specific values in the sense that similarly looking diagrams are obtained for a wide range of parameter choices in addition to the above ones [41].